Localized excitons in II-VI semiconductor alloys: Density-of-states model and photoluminescence line-shape analysis

Djamel Ouadjaout and Yves Marfaing
Laboratoire de Physique des Solides de Bellevue, Centre National de la Recherche Scientifique, 92195 Meudon CEDEX, France
(Received 2 January 1990)

A simple but tractable model of the density of exciton states associated with potential fluctuations in semiconductor alloys is proposed. It consists of minimizing the fluctuation entropy related to the composition fluctuation Δx averaged over a volume V, for a given localization energy ε. A critical volume $V_c(\Delta x)$, defined as the smallest volume in which the fluctuation Δx can occur, is introduced. This model leads to a density-of-states tail of the form $\exp[-(\varepsilon/\varepsilon_0)^{3/2}]$. The characteristic energy ε_0 depends on the manner an exciton can be localized: as a whole or through electron and/or hole confinement. It is shown that the most probable event is determined by two physical parameters of the system: the electron-hole mass ratio and the ratio between the coefficients of variation with composition of the conduction- and valence-band edges. The density of states is used to model the exciton photoluminescence line shape of three representative alloys $Zn_{0.97}Hg_{0.03}Te$, $CdS_{0.36}Se_{0.64}$, and $Cd_{0.92}Hg_{0.08}Te$ in which exciton localization occurs, respectively, via the electron, via the hole, or by electron-hole confinement. In each case a good agreement with the experimental results is obtained.

I. INTRODUCTION

The problem of exciton localization in semiconductor alloys has been a subject of continuous interest since the first works of Cohen and Sturge[1] and Permogorov *et al.*[2] The more specific results have been obtained in II-VI semiconductor alloys situated on the high-band-gap side of the composition range, including CdS_xSe_{1-x}, ZnS_xSe_{1-x}, $Cd_xHg_{1-x}Te$, and $Zn_xHg_{1-x}Te$. In that case the low temperature photoluminescence spectra are dominated by a band located below the free-exciton reflectivity structure. This band is interpreted as the recombination of excitons in a tail of states associated with alloy fluctuations. Time-resolved photoluminescence experiments have been used to study the transfer of excitation between localized states in the tail.[3-5]

On the other hand, the behavior of alloys corresponding to the low-band-gap side of the composition range appears to be somewhat different. The photoluminescence spectra show the usual donor- and acceptor-bound exciton recombination lines, broadened by alloy fluctuations and, at higher energy, a narrow line which has been related to free-exciton or polariton annihilation in the following alloys: $Zn_xCd_{1-x}Te$, $Zn_{1-x}Mg_xSe$, $ZnSe_xTe_{1-x}$, $CdSe_xTe_{1-x}$ (Ref. 6), and also CdS_xSe_{1-x}.[7] However, in the case of ZnCdS (Ref. 8) and ZnCdSe (Ref. 9) the high-energy line was still interpreted in terms of shallow localized states.

From the theoretical point of view, the first aspect to be considered is the modification of the exciton density of states due to alloying. Baranovski and Efros[10] first treated this problem by looking for the optimal composition fluctuation Δx which gives a minimum in the fluctuation entropy for a given localization energy ε. They arrived at a tail of the density of states varying as $\exp[-(\varepsilon/\varepsilon_0)^{1/2}]$ where ε_0 is a characteristic energy. Cohen and Sturge[1] made reference to the work of Halperin and Lax[11] on a related problem, the impurity band tails. This study led to a density of states of the form $\exp[-(\varepsilon/\varepsilon_0)^{a(\varepsilon)}]$ where the exponent $a(\varepsilon)$ varies from 0.5 to 2 with increasing localization energy. A simpler expression with $a=1$ was adopted by Cohen and Sturge in their line-shape analysis. The same form was chosen in subsequent theoretical modelings of time-resolved and -integrated luminescence spectra.[5,12] In these studies the characteristic energy of the tail ε_0 was not calculated *a priori* but taken as a fitting parameter.

Our own effort was directed towards the derivation of a physically meaningful, but tractable model of the density of states which allows us a comparison between the various alloys in terms of a few fundamental quantities.

This simple model is presented in the first part of this paper. Then, the obtained expressions are used to evaluate the relative probabilities of different possible electronic excitations: exciton localized as a whole, exciton localized through one of its components (electron or hole), and exciton in narrow wells. At last these predictions are confronted to experimental results by modeling the steady-state photoluminescence band observed in three different exemplary alloys: $Zn_{0.97}Hg_{0.03}Te$, $Cd_{0.92}Hg_{0.08}Te$, and $CdS_{0.36}Se_{0.64}$.

II. MODEL OF THE DENSITY OF EXCITON STATES INDUCED BY COMPOSITION FLUCTUATIONS

Consider a pseudobinary semiconductor alloy of nominal formula $A_{1-x_0}B_{x_0}C$ where x_0 denotes the average composition. At the microscopic level the random distribution of atoms A and B on the same sublattice generates

local composition fluctuations. If in a small volume V the average composition is ξ, the corresponding composition fluctuation is

$$\Delta x(V)=\xi(V)-x_0 \ . \tag{1}$$

We are interested in the relative probability $p(\Delta x, V)$ of occurence of the composition fluctuation Δx in the volume V.

To express it we refer to the statistical formalism of Lifshitz[13] who writes the density of fluctuation entropy as

$$\frac{dS(\xi)}{dV}=\frac{\sigma(\xi)-\sigma(x_0)-(\xi-x_0)\sigma'(x_0)}{V_c} \ , \tag{2}$$

where $\sigma(x)=-x\ln x-(1-x)\ln(1-x)$. V_c is the interaction volume of the perturbation. In their study, Baranovski and Efros take V_c equal to the volume of a sublattice site.[10] Following Singh and Bajaj[14] we take V_c as the smallest volume in which a fluctuation Δx can occur. It is given by

$$K|\Delta x|V_c=1 \ , \tag{3}$$

where K is the concentration of sublattice sites. The entropy of the fluctuation in the volume V is obtained by integrating Eq. (2). In our simple model we write

$$S(\xi)=\frac{V}{V_c}[\sigma(\xi)-\sigma(x_0)-(\xi-x_0)\sigma'(x_0)] \ . \tag{4}$$

From the general relation between configuration probability and entropy $p\sim\exp(-S)$, we obtain after some transformations:

$$p(\xi,V)\simeq\exp\left\{-\frac{V}{V_c}\left[\xi\ln\left[\frac{\xi}{x_0}\right]+(1-\xi)\ln\left[\frac{1-\xi}{1-x_0}\right]\right]\right\} \ . \tag{5}$$

In the approximation of small fluctuations, $|\Delta x|\ll\min(x_0,1-x_0)$, which corresponds generally to the experimental cases, the expression (5) becomes similar to a Gaussian distribution with a standard deviation $\sigma_0=[(V_c/V)x_0(1-x_0)]^{1/2}$. Introducing the relation (3), the configuration probability is finally expressed as

$$p(\Delta x,V)\sim\exp\left[-\frac{KV|\Delta x|^3}{x_0(1-x_0)}\right] \ . \tag{6}$$

The next step is to relate the local composition fluctuation $(\Delta x, V)$ to the energy spectrum of excitons in the semiconductor. The basic idea is that, at low temperatures, excitons are localized in potential wells associated with composition fluctuations. However, depending on the extension of the wells and on the fluctuation amplitude different kinds of exciton localization can be considered, namely the following: (i) localization of the exciton as a single particle in a well of radius larger than the exciton Bohr radius, (ii) localization of one of the exciton components (electron or hole), the other particle being bound by coulombic interaction, and (iii) quantum localization of both exciton components in a narrow well leading to a confined exciton. The two first cases can be treated on the same foot and will be studied first.

A. One-particle localization

Besides the separate localization of either an electron or a hole, this case covers the situation where the exciton can be treated as a simple particle of mass equal to the exciton translation mass $M=m_n^*+m_p^*$ (center-of-mass localization). The necessary condition is that the localization energy is a small perturbation compared to the exciton binding energy, as indicated by Baranovski and Efros.[10] This case also corresponds to the quantification of excitonic polaritons in wide two-dimensional wells (≥ 500 Å) analyzed by Merle d'Aubigné *et al.* in CdZnTe/CdTe/CdZnTe quantum structures.[15]

We consider the energy configuration of Fig. 1 relevant to a localized exciton. The particle of mass M is localized at an energy ε below the threshold energy E_X in a (supposed) spherical potential well of radius R and of depth ΔE. θ is the kinetic energy of confinement, a function of M, ΔE, and R. E_X is the free-exciton energy corresponding to the average composition x_0. The recombination energy is then $h\nu=E_X-\varepsilon$. We can write

$$\Delta E=\varepsilon+\theta=-\alpha_X\,\Delta x \ , \tag{7}$$

where $\alpha_X=dE_X/dx$ is the coefficient of variation of the excitonic band gap with composition. The fluctuations Δx considered are such as $\Delta E>0$.

For a given localization energy ε, ΔE and R can be chosen to maximize the probability $p(\Delta x, V)$, (6), by solving

$$\frac{d}{dR}(R^3|\Delta x|^3)=\frac{d}{dR}\left[\frac{R^3(\varepsilon+\theta)^3}{|\alpha_X|^3}\right]=0 \ . \tag{8}$$

This procedure determines the optimum fluctuation parameters $\Delta E_{\rm op}$ and $R_{\rm op}$. In the approximation of a spherical potential well, the kinetic energy θ is related to ε and R by the well known transcendental equation written in dimensionless variables:[16]

$$\cot(\sqrt{2Z})=-\sqrt{Y/Z} \ , \tag{9}$$

where $Z=\theta MR^2/\hbar^2$ and $Y=\varepsilon MR^2/\hbar^2$. We have fitted the solution of (9) in the range of interest by a third degree polynomial:

$$Z=\sum_{n=0}^{3}\omega_n(\sqrt{Y})^n \ . \tag{10}$$

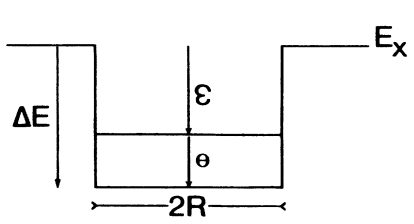

FIG. 1. Scheme of one-particle localization in a spherical potential well.

Figure 2 presents the adjustment obtained with the coefficients $\omega_0=1.2642$, $\omega_1=1.2656$, $\omega_2=-0.2462$, and $\omega_3=0.0193$. Introducing (10) in (8) leads to the optimum parameters:

$$R_{\rm op}=1.4\frac{\hbar}{\sqrt{M}\,\varepsilon}\ , \tag{11a}$$

$$\Delta E_{\rm op}=2.33\varepsilon=4.567\frac{\hbar^2}{MR_{\rm op}^2}\ . \tag{11b}$$

Then the density of states at the energy ε in the tail is taken to be proportional to the probability $p(R_{\rm op},\Delta E_{\rm op})$. We find

$$g(\varepsilon)=g_0\exp\left[-\left[\frac{\varepsilon}{\varepsilon_0}\right]^{3/2}\right]\ , \tag{12}$$

where ε_0 is a characteristic energy given by

$$\varepsilon_0=\frac{3^{2/3}}{(1.4\times2.33)^2(4\pi)^{2/3}}\frac{M\alpha_g^2[x_0(1-x_0)]^{2/3}}{\hbar^2K^{2/3}}\ . \tag{13}$$

We have introduced $\alpha_g=dE_g/dx=\alpha_X$, where E_g is the energy band gap which amounts to neglecting the variation of exciton binding energy with composition x. The value of the constant first factor is about $\frac{1}{28}$. If we consider instead the localization of an electron or a hole the product $M\alpha_g^2$ is replaced by the quantity $m_n^*\alpha_n^2$ or $m_p^*\alpha_p^2$ respectively, where m_n^* (m_p^*) is the electron (hole) effective mass and α_n (α_p) is the variation rate of the conduction- (valence-) band edge with composition. In the latter cases the localized energy ε is referred to the corresponding continuum edge, either the conduction- or the valence-band edge. By considering that the localization particle attracts a (delocalized) carrier of opposite sign to form an exciton the recombination energy is still given by $h\nu=E_X-\varepsilon$.

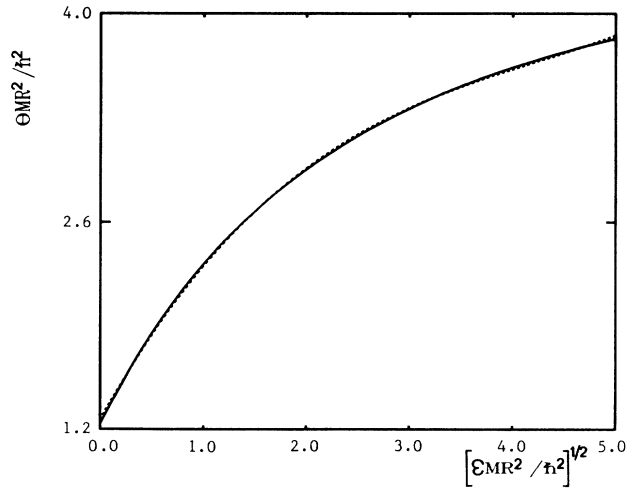

FIG. 2. The dimensionless kinetic energy plotted vs the dimensionless localization energy for a particle of mass M in a spherical potential well: solid line, exact solution; dashed line, approximation by a third-degree polynomial (see text).

B. Two-particle localization

When the perturbation due to localization is greater than the electron-hole interaction energy, one has to treat first the localization of both particles before introducing electron-hole Coulombic interaction. We assume that the potential wells are distant enough to consider the two particles to be confined in the same well of radius R (Fig. 3). Then we can write

$$\Delta E_n=-\alpha_n\,\Delta x=\varepsilon_n+\theta_n\ , \tag{14a}$$

$$\Delta E_p=+\alpha_p\,\Delta x=\varepsilon_p+\theta_p\ , \tag{14b}$$

$$\Delta E_g=-(\alpha_n-\alpha_p)\Delta x=-\alpha_g\,\Delta x=\varepsilon+\theta_n+\theta_p\ , \tag{14c}$$

$$h\nu=E_g-E_{BX}-\varepsilon\ . \tag{14d}$$

The recombination energy is related to the total localization energy ε and involves the exciton binding energy E_{BX}. As a first approximation we assume that E_{BX} does not depend on R. As above the possible fluctuations Δx leading to localization are such as $\Delta E_n>0$ and $\Delta E_p>0$.

The optimum fluctuation for a given ε value is determined by solving Eq. (8). In this case it is more convenient to express the kinetic energies θ_n and θ_p as a function of R and of the potential depths ΔE_n and ΔE_p. The equation of the spherical potential well (9) is solved to give Z as a function of $X=Z+Y$, where $X=\Delta E\,MR^2/\hbar^2$. We have approximated the solution by a second-degree polynomial as shown in Fig. 4. We write

$$Z=\sum_{m=0}^{2}a_mX^m \tag{15}$$

with $a_0=0.3813$, $a_1=0.8537$, and $a_2=-0.0802$. This simple form can now be introduced into Eqs. (14a), (14b), and (14c) to get a relation between Δx, R, and ε, where Δx appears at the second order only. Substituting the solution for Δx in (8) allows one to determine the parameters of the optimum fluctuation for a given localization

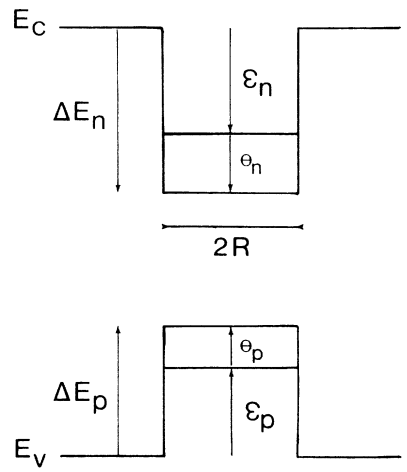

FIG. 3. Scheme of electron and hole localization in a spherical potential well.

energy ε:

$$R_{op}=a_0^{1/2}\left[1-\frac{u}{\Omega}\right]^{1/2}\frac{\hbar}{\sqrt{\mu\varepsilon}}\ ,$$
$$\Delta x_{op}=\frac{2\varepsilon}{(1-a_1)(1-u/\Omega)\alpha_g}\ , \tag{16}$$

with

$$u=\frac{(a_n^2 m_n^*+\alpha_p^2 m_p^*)}{\mu\alpha_g^2}\ ,$$
$$\Omega=\frac{(1-a_1)^2}{4a_0a_2}=-0.228\ , \tag{17}$$

where μ is the reduced exciton mass [$\mu=(1/m_n^*+1/m_p^*)^{-1}$].

The density of states in the tail, proportional to $p(R_{op},\Delta x_{op})$, keeps the same form as above (12), but now with

$$\varepsilon_0=\gamma(u)\frac{\mu\alpha_g^2[x_0(1-x_0)]^{2/3}}{\hbar^2K^{2/3}}\ , \tag{18}$$

where

$$\gamma(u)=\left[\frac{3}{4\pi}\right]^{2/3}a_2u\left[\frac{\Omega}{u}-1\right]\ , \tag{19}$$

The previous case of one-particle localization can be also obtained from (18) and (19), by setting $u=1$ and introducing the appropriate mass and band variation coefficient; then $\gamma(1)=\frac{1}{28}$.

In the model of density of states developed above, the alloy characteristics are represented by five quantities depending on the composition x_0: K, m_n^*, m_p^*, α_n, and α_p. The last four parameters determine the type and the degree of localization that excitons can exhibit in the studied alloy. In this respect we will show in the next section that the various alloys can be classified according to two quantities only: the ratio m_n^*/m_p^* and α_n/α_p.

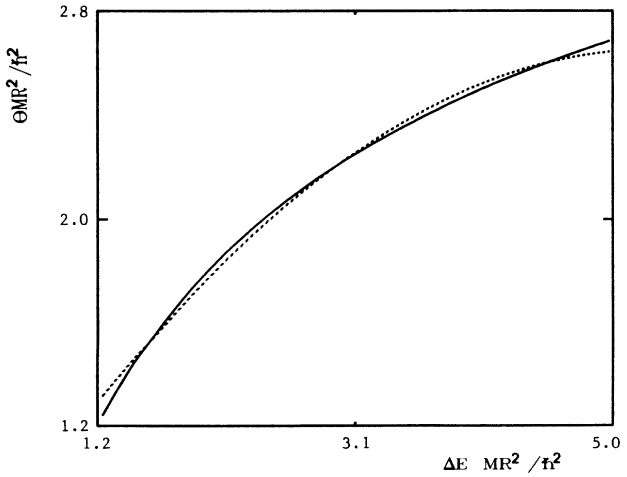

FIG. 4. The dimensionless kinetic energy plotted vs the dimensionless potential depth for a particle of mass M in a spherical well: solid line, exact solution; dashed line, approximation by a second-degree polynomial (see text).

III. TYPES OF EXCITON LOCALIZATION IN II-VI SEMICONDUCTOR ALLOYS

Except for the study of Ablyazov *et al.*,[17] we are not aware of any general discussion about the possible kinds of exciton localization in II-VI semiconductor alloys. Our simple model allows us to establish the conditions of existence and relative probabilities of the different kinds of electronic excitations in terms of only a few parameters. In the following, three categories of alloys will be defined according to the nature of the localized particle. Each category will be represented by a typical alloy for which experimental results have been obtained or are known from the literature.

A. Electron localization

The optimum fluctuation parameters are obtained from (11):

$$R_n=1.4\frac{\hbar}{(m_n^*\varepsilon)^{1/2}}\ , \tag{20}$$

A necessary condition of validity is that the hole is *not* localized in that well. Then the hole potential well has to satisfy

$$\Delta E_p=\alpha_p\,\Delta x<\frac{\pi^2}{8}\frac{\hbar^2}{m_p^*R_n^2}\ , \tag{21}$$

which is the localization criterion for a spherical well. From (20) and (21) we deduce the explicit condition

$$-\frac{\alpha_p}{\alpha_n}<\frac{1}{3.7}\frac{m_n^*}{m_p^*}\ . \tag{22}$$

Note that this inequality is always satisfied in the case $(-\alpha_n/\alpha_p)<0$.

Another requirement is that this type of excitation has the highest probability of occurence compared to the other ones (hole localization and exciton confinement). This comes down to make maximum the corresponding density of states at a given energy ε and consequently the characteristic energy ε_0. From (18) this is written as

$$\gamma(1)\alpha_n^2m_n^*>\max\{\gamma(1)\alpha_p^2m_p^*,\gamma(u)\alpha_g^2\mu\}\ . \tag{23}$$

Two cases are worth considering. If $(-\alpha_n/\alpha_p)>0$ the above condition is equivalent to (22). If $(-\alpha_n/\alpha_p)<0$, the possibility of localizing an electron and a hole in the same disorder-induced well is excluded, and (23) is reduced to

$$\frac{\alpha_n}{\alpha_p}>\left[\frac{m_p^*}{m_n^*}\right]^{1/2}\ . \tag{24}$$

B. Hole localization

This case is symmetrical to the previous one. Therefore, the necessary condition of validity is

$$-\frac{\alpha_n}{\alpha_p} < \frac{1}{3.7}\frac{m_p^*}{m_n^*} \quad . \tag{25}$$

This inequality is always satisfied for $(-\alpha_n/\alpha_p)<0$.

The condition of maximum probability reads

$$\gamma(1)\alpha_p^2 m_p^* > \max\{\gamma(1)\alpha_n^2 m_n^*, \gamma(u)\alpha_g^2\mu\} \quad . \tag{26}$$

In the case $(-\alpha_n/\alpha_p)<0$, for the same reasons as above, (26) becomes

$$\frac{\alpha_n}{\alpha_p} < \left[\frac{m_p^*}{m_n^*}\right]^{1/2} \quad . \tag{27}$$

For the other case $(-\alpha_n/\alpha_p)>0$ the conditions (25) and (26) are simultaneously satisfied if the following inequality applies:

$$P_q(s,t)=\sum_{q=0}^{4} C_q(t)s^q<0 \quad . \tag{28}$$

Where we set $t=m_n^*/m_p^*$, $s=-\alpha_n/\alpha_p$, and the coefficients C_q are defined by

$$\begin{aligned} C_0(t)&=\Lambda\left[\Omega-\frac{1}{t}\right]-\frac{1}{t}-1 \ , \\ C_1(t)&=2\Lambda\Omega \ , \\ C_2(t)&=\Lambda(\Omega-1-t)+\Lambda t\left[\Omega-\frac{1}{t}-1\right]-1-t \ , \\ C_3(t)&=2\Lambda\Omega t \ , \\ C_4(t)&=\Lambda t(\Omega-1-t) \ . \end{aligned} \tag{29}$$

Ω is defined in (17), and $\Lambda=2.66a_2 8^{2/3}=-0.81$.

C. Exciton confinement

Electron and hole are both localized in the same well, which implies $(-\alpha_n/\alpha_p)>0$. The conditions of existence are

$$\begin{aligned} -\alpha_n\Delta x &> \frac{\pi^2}{8}\frac{\hbar^2}{m_n^* R^2} \ , \\ \alpha_p\Delta x &> \frac{\pi^2}{8}\frac{\hbar^2}{m_p^* R^2} \ . \end{aligned} \tag{30}$$

With the optimum R and Δx values given in (16), we get the following equivalent inequalities:

$$\left[\frac{16a_0[1+(m_n^*/m_p^*)]}{\pi^2(1-a_1)}-1\right]^{-1} < -\frac{\alpha_n}{\alpha_p} < \left[\left[1+\frac{m_p^*}{m_n^*}\right]\frac{16a_0}{\pi^2(1-a_1)}-1\right] \quad . \tag{31}$$

The condition of maximum probability is

$$\gamma(u)\mu\alpha_g^2 > \max\{\gamma(1)m_n^*\alpha_n^2, \gamma(1)m_p^*\alpha_p^2\} \quad . \tag{32}$$

The combination of the three conditions (31) and (32) leads to the following result:

$$\begin{aligned} -\frac{\alpha_n}{\alpha_p} &< 3.7\frac{m_p^*}{m_n^*} \ , \\ P_q(s,t) &> 0 \ , \end{aligned} \tag{33}$$

where P_q is defined by (28) and (29).

D. Center-of-mass exciton localization

This situation can occur whatever the sign of $(-\alpha_n/\alpha_p)$. It was not opposed to the previous ones because of its particular validity range. It corresponds to a weak localization regime such as

$$R \gg a_B^* = \left[\frac{\hbar^2}{2\mu E_{BX}}\right]^{1/2} \ , \tag{34}$$

where a_B^* is the exciton Bohr radius and E_{BX} the exciton binding energy. Taking into account the expression (11a) of the optimum fluctuation radius, the condition (34) becomes

$$\frac{\varepsilon}{E_{BX}} \ll \frac{1.4}{1+(m_n^*/2m_p^*)+(m_p^*/2m_n^*)} \quad . \tag{35}$$

As m_n^*/m_p^* is typically around 0.2 the above inequality requires that ε is much smaller than the exciton binding energy. Practically this corresponds to a small part of the observed luminescence bands, about 2–3 meV below the free-exciton energy, and is completely absent in the small-band-gap alloys. Thus this process will not be considered any more for the modeling of luminescence spectrum (Sec. IV).

E. Summary and examples

The conditions of appearance of the different types of exciton localization expressed in the previous section can be represented by limit curves in a graph relating $(-\alpha_n/\alpha_p)$ to (m_n^*/m_p^*) (Fig. 5). The expressions (22), (28), and (33) corresponding to the case $-\alpha_n/\alpha_p>0$ allow one to delimit three domains: The upper domain (EL) corresponds to alloys where conduction-band fluctuations are much larger than valence-band fluctuations $(\alpha_n \gg -\alpha_p)$, which leads to electron localization. A prototype of this class is $Zn_xHg_{1-x}Te$ $(0.9<x<1)$ for which the coefficient α_p was recently determined by photoemission and is near zero.[18] The lower domain (HL) covers the opposite situation where the hole is localized

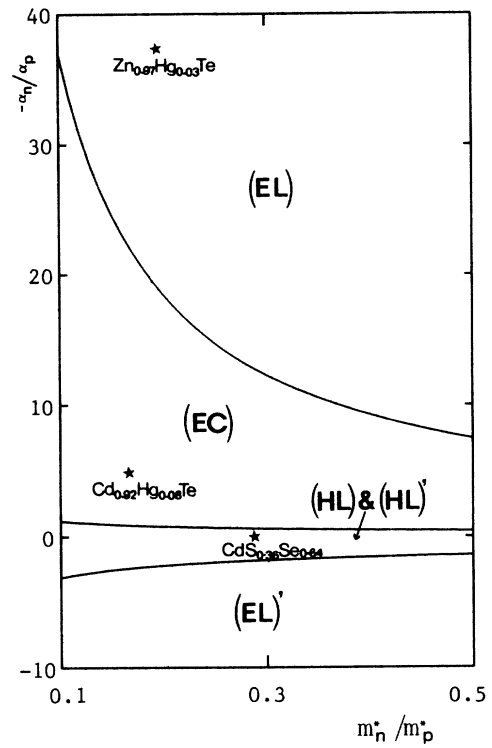

FIG. 5. Graph relating the ratio of the coefficients of variation of band edges with composition to the electron-hole mass ratio. The domains (EL) and (EL)' correspond to electron localization, (HL) and (HL)' to hole localization and (EC) to exciton confinement.

in potential fluctuations. A representative alloy is CdS_xSe_{1-x} $(0.3<x<0.97)$ for which α_n is quite small (see Sec. V). The intermediate domain (EC) corresponds to excitons confined in narrow wells. This appears to apply to the alloy $Cd_xHg_{1-x}Te$ $(0.8<x<1)$ because $-\alpha_p$ is not negligible compared to α_n as it was the case for $Zn_xHg_{1-x}Te$. Hence, localization of both electron and hole occurs in potential fluctuations.

For the case $(-\alpha_n/\alpha_p)<0$, two domains are delimited by the conditions (24) and (27). In the lower part of Fig. 5 the domain (EL)' corresponds to electron localization and the domain (HL)' corresponds to hole localization as the adjacent domain (HL) does.

To go a step further we will now use our model of density of states to fit the spectral distribution of the photoluminescence bands observed in three typical alloys previously mentioned.

IV. PHOTOLUMINESCENCE LINE-SHAPE MODELING

We consider a steady-state nonresonant type of excitation: Photons of energy higher than the semiconductor band gap contribute to establish a population of free excitons of density n_0, from which capture to localized states proceeds. In the small-excitation regime and at sufficiently low temperatures, the density of localized excitons at energy ε satisfies the rate equation:

$$\beta n_0 g(\varepsilon)+\sum_{\varepsilon'=0}^{\varepsilon} W_{\varepsilon'\to\varepsilon}(\varepsilon',\varepsilon)n(\varepsilon')-\frac{n(\varepsilon)}{\tau(\varepsilon)}=0 . \quad (36)$$

The first term is the total capture rate including the direct capture and the indirect one involving scattering on states of intermediate energy $\varepsilon'<\varepsilon$. The effective capture coefficient β is assumed not to depend on ε. The second term represents phonon-assisted tunneling from states localized at energy $\varepsilon'<\varepsilon$. The last term includes all the processes of state emptying: radiative recombination and transfer to states deeper in the tail. The lifetime $\tau(\varepsilon)$ can be decomposed in a radiative $\tau_R(\varepsilon)$ and a transfer component $\tau_{tr}(\varepsilon)$:

$$\tau^{-1}(\varepsilon)=\tau_R^{-1}(\varepsilon)+\tau_{tr}^{-1}(\varepsilon) \quad (37)$$

with

$$\tau_{tr}^{-1}(\varepsilon)=\sum_{\varepsilon'=\varepsilon}^{\infty} W_{\varepsilon'\to\varepsilon'}(\varepsilon,\varepsilon') . \quad (38)$$

The transfer probability W can be evaluated exactly by formulating the exciton-phonon interaction.[1,5]

For the sake of simplicity, we have followed the phenomenological model of Ref. 12. These authors assume that $W(\varepsilon,\varepsilon')$ has the simple form

$$W(\varepsilon,\varepsilon')=W_0(\varepsilon)g(\varepsilon') . \quad (39)$$

Furthermore they express the transfer rate $\tau_{tr}^{-1}(\varepsilon)$ as

$$\tau_{tr}^{-1}(\varepsilon)=\tau_R^{-1}\exp[\delta(\varepsilon_M-\varepsilon)] , \quad (40)$$

where ε_M is a reference energy at which the radiative recombination probability is equal to the transfer probability.

Here τ_R is taken as a constant, independent of energy. One can argue that with increasing localization energy the radius R of the optimum fluctuation decreases so that the exciton oscillator strength which scales as R^3 (Ref. 19) should also decrease. However, taking into account the small energy range of the luminescence bands (about 10–20 meV), we will neglect this variation before that of the transfer probability. Then the expression of the lifetime is

$$\tau^{-1}(\varepsilon)=\tau_R^{-1}\{1+\exp[\delta(\varepsilon_M-\varepsilon)]\} . \quad (41)$$

Introducing formulas (39) and (40) into (38) and replacing the summation by an integral allows one to obtain the probability coefficient

$$W_0(\varepsilon)=\frac{\tau_R^{-1}\exp[\delta(\varepsilon_M-\varepsilon)]}{\int_{\varepsilon}^{\infty} g(\varepsilon')d\varepsilon'} , \quad (42)$$

and to write (36) under the form

$$\frac{n(\varepsilon)}{\tau(\varepsilon)}=\beta n_0 g(\varepsilon)+\int_0^{\varepsilon} W_0(\varepsilon')n(\varepsilon')g(\varepsilon)d\varepsilon' . \quad (43)$$

This equation can be solved by successive iterations as follows: The first two steps give

$$n_0(\varepsilon)=\beta n_0 g(\varepsilon)\tau(\varepsilon) ,$$

$$n_1(\varepsilon)=n_0(\varepsilon)[1+A(\varepsilon)] ,$$

where

$$A(\varepsilon)=\int_0^{\varepsilon} W_0(\varepsilon')g(\varepsilon')\tau(\varepsilon')d\varepsilon' \ . \tag{44}$$

At the second order we get

$$n_2(\varepsilon)=n_0(\varepsilon)\left[1+A(\varepsilon)+\int_0^{\varepsilon} W_0(\varepsilon')g(\varepsilon')\tau(\varepsilon')A(\varepsilon')d\varepsilon'\right] .$$

By noting that

$$W_0(\varepsilon')g(\varepsilon')\tau(\varepsilon')=\frac{dA(\varepsilon')}{d\varepsilon'} ,$$

the second-order solution reads

$$n_2(\varepsilon)=n_0(\varepsilon)[1+A(\varepsilon)+\tfrac{1}{2}A^2(\varepsilon)] .$$

Extending this process to the order n leads to the exact solution:

$$n(\varepsilon)=n_0(\varepsilon)\exp[A(\varepsilon)] . \tag{45}$$

The luminescence intensity due to the radiative recombination of the excitons localized at energy ε is $I_L(\varepsilon)=n(\varepsilon)/\tau_R$:

$$I_L(\varepsilon)=\beta n_0 g(\varepsilon)\tau(\varepsilon)\tau_R^{-1}\exp[A(\varepsilon)] . \tag{46}$$

The expression (46) was used to fit the low-temperature luminescence bands observed in three representative alloys by us or other authors: $Zn_{0.97}Hg_{0.03}Te$, $Cd_{0.92}Hg_{0.08}Te$,[20] and $CdS_{0.36}Se_{0.64}$.[5] The experimental spectra were plotted as a function of the localization energy ε by subtracting the photon energy from the free-exciton energy (14d). The latter was reduced from reflectivity measurements in the case of $Cd_xHg_{1-x}Te$ (Ref. 21) and CdS_xSe_{1-x} (Ref. 5) or calculated by linearly interpolating the reflectivity results obtained on some Zn-rich $Zn_xHg_{1-x}Te$ alloys.[22]

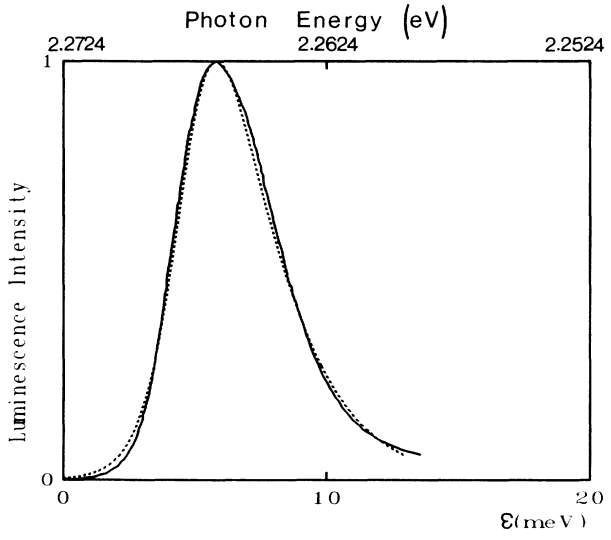

FIG. 6. Comparison between the experimental luminescence spectrum (solid line) and the calculated one (dashed line) computed from the model presented in Sec. IV for $Zn_{0.97}Hg_{0.03}Te$.

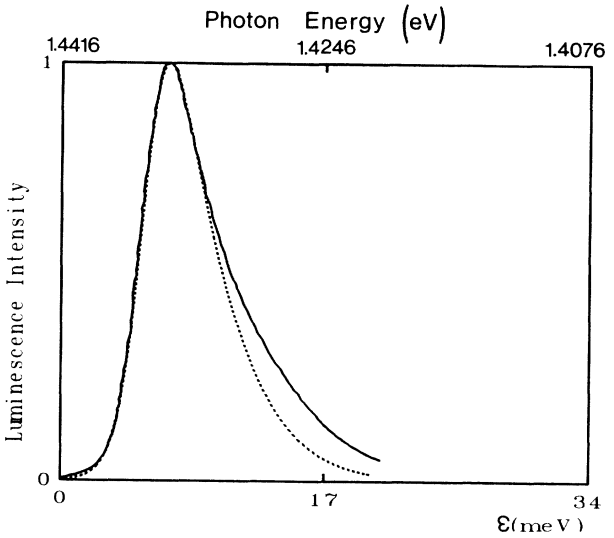

FIG. 7. Comparison between the experimental luminescence spectrum (solid line) and the calculated one (dashed line) computed from the model presented in Sec. IV for $Cd_{0.92}Hg_{0.03}Te$.

As the luminescence curves are normalized to their maximum, the fits involve only three parameters: ε_0 the characteristic energy of the density of states (12), δ, and ε_M, which determine the lifetime variation (38).

A simple procedure is to adjust first the position of the curve peaks which gives a relation between ε_0, ε_M, and δ. The short wavelength range (small ε) is quite sensitive to the lifetime variation, while the long wavelength side (large ε) is mainly determined by the density-of-states expression (ε_0). The best fits obtained are presented in Figs. 6, 7, and 8 as dashed lines together with the experimental results (solid lines). The fitting parameters for the three curves are collected in Table I. The experimental value of the characteristic energy ε_0 is compared to the theoretical one in the next section.

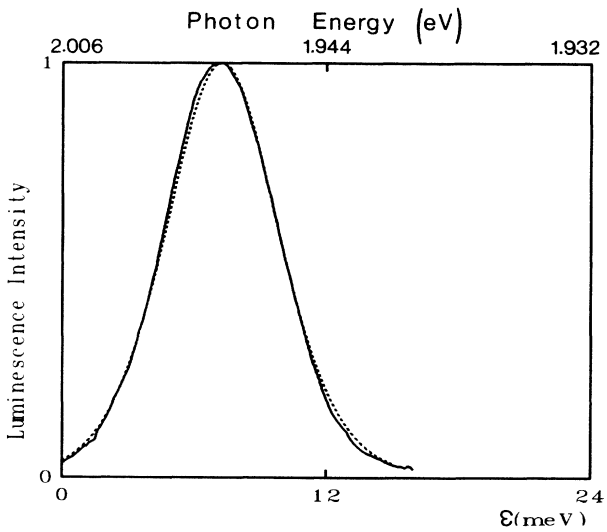

FIG. 8. Comparison between the experimental luminescence spectrum (solid line) and the calculated one (dashed line) computed from the model presented in Sec. IV for $CdS_{0.36}Se_{0.64}$.

TABLE I. Best parameters used for the fit of the experimental luminescence spectra according to the theoretical model of Sec. IV.

	$Zn_{0.97}Hg_{0.03}Te$	$CdS_{0.36}Se_{0.64}$	$Cd_{0.92}Hg_{0.08}Te$
ε_0 (meV)	4.8	4.3	6.5
δ (meV^{-1})	1.23	0.56	1.15
ε_M (meV)	4.7	6.7	5.5

V. DISCUSSION OF THE RESULTS

The validity of our model for the density of localized states can be appreciated from a comparison between the ε_0 experimental values and the predicted ones. The latter are evaluated by introducing the relevant alloy parameters in the appropriate expressions of Sec. II. These parameters are listed in Table II and come from various sources. The effective masses are linearly interpolated between the accepted values of the end compounds.[23] In the same way K is calculated from linearly interpolated lattice parameters.[23] The band-edge coefficients for $Zn_xHg_{1-x}Te$ alloys are estimated by assuming that E_c is a linear function of x and that $E_v(x)$ follows the nonlinear dependence recently measured[18] making a valence band offset of 0.17 eV appear between ZnTe and HgTe. For $Cd_xHg_{1-x}Te$ alloys a linear variation $E_v(x)$ has been assumed with a valence-band offset of 0.35 eV between CdTe and HgTe;[24] then the dependence $E_c(x)$ was deduced from the band-gap variation given by Legros *et al.*[25] In the case of CdS_xSe_{1-x} alloys the conduction-band offset is taken to be zero as an average value between calculated (Harrison) and experimental (Swank) values of opposite signs.[26] Then the variation $E_v(x)$ follows the quadratic dependence of the band gap with composition.[27]

For $Zn_{0.97}Hg_{0.03}Te$ and $CdS_{0.36}Se_{0.64}$ the conditions of one-particle localization apply, electron, (22), and hole localization, (28), respectively: ε_0 is computed from (13) with the corresponding parameters. In the case of $Cd_{0.92}Hg_{0.08}Te$ the condition of two-particle localization or exciton confinement is obeyed, (33), and ε_0 is calculated from the formula (18). Comparison between Table I and Table II shows that the predicted ε_0 values are in good agreement with the experimental ones. Note in particular that $Zn_xHg_{1-x}Te$ and CdS_xSe_{1-x} correspond to two opposite cases of localization. As for $Cd_xHg_{1-x}Te$ the accuracy of the fit on the long wavelength side (large ε) is limited by the presence of another luminescence band not represented here, which introduces some uncertainty in the actual band shape. The bottom lines of Table II indicate the parameters of the optimum fluctuations corresponding to the peak luminescence energy.

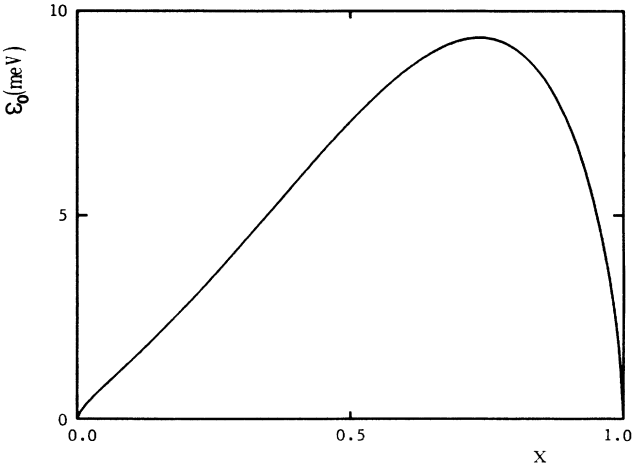

FIG. 9. Composition dependence of the characteristic energy ε_0 of the density of localized exciton states (13) for CdS_xSe_{1-x} alloys.

On the whole our model appears to represent fairly well the different physical situations studied here. It gives the characteristic energy of band tailing with an accuracy never previously obtained. In this respect it is instructive to come back to the analysis of Baranovski and Efros.[10] These authors have determined the optimum fluctuation in using a more rigorous quantum-mechanical formulation. However, they did not introduce a critical volume V_c depending on composition fluctuation (3): their calculation is equivalent to taking $V_c = K^{-1}$. This procedure leads to a density of states proportional to $\exp[-(\varepsilon/\varepsilon_0)^{1/2}]$. A reasonable fit of the experimental luminescence bands is also possible with this form, leading to ε_0 values around 3–4 meV. However, introducing the alloy parameters of Table II in the formula of Ref. 10

TABLE II. Lattice and band-structure parameters of the considered alloys. The three last lines give the calculated values of the density of states characteristic energy and the optimum fluctuation parameters.

	$Zn_{0.97}Hg_{0.03}Te$	$CdS_{0.36}Se_{0.64}$	$Cd_{0.92}Hg_{0.08}Te$
K (10^{22} cm^{-3})	1.76	1.88	1.47
m_n^*/m_0	0.11	0.14	0.093
m_p^*/m_0	0.594	0.5	0.584
α_n (eV)	2.52	0	1.9
α_p (eV)	−0.067	−0.64	−0.35
ε_0 (meV)	4.6	5.2	5.9
R_{op} (Å)	153	64.5	168.9
Δx_{op}	-5.4×10^{-3}	-2.6×10^{-2}	-7.7×10^{-3}

gives ε_0 theoretical values 2 to 3 orders of magnitude smaller. We conclude that the concept of a fluctuation-dependent critical volume is a necessary ingredient in this type of formulation. Another aspect to be discussed concerns the II-VI semiconductor alloys near the small-band-gap side for which a different type of luminescence spectrum is observed. As indicated in the introduction, the spectrum is rather similar to that of the near compound. At low temperature donor- and acceptor-bound exciton lines appear together with an intense narrow line very close to the free-exciton energy E_X. We will consider more specifically the alloy $CdS_{0.14}Se_{0.86}$ well studied in Ref. 7 and discuss the particular observed behavior by comparison with the composition $CdS_{0.36}Se_{0.64}$ analyzed above in terms of localized excitons. We wish to show that these two different behaviors can be related to the density of localized states at the energy of the donor-bound exciton. Taking a density of states of the form

$$g(\varepsilon)=g_0 \exp[-(\varepsilon/\varepsilon_0)^{3/2}] ,$$

we note that ε_0 varies as a function of x as shown in Fig. 9. The calculation was made using the expression (13) in the framework of hole localization. The quantity g_0 is estimated by matching it to the free-exciton-state density $g_f(E)$ at some energy E_S above E_X.[28] g_f is given by

$$g_f=4\pi\left[\frac{2M}{h^2}\right]^{3/2}(E-E_X)^{1/2} ,$$

where M is the exciton translational mass. Somewhat arbitrarily we take $E_S-E_X=\varepsilon_0/2$. With that we calculate $g_0=1.98\times10^{20}$ $eV^{-1}cm^{-3}$ for $x_S=0.36$ and $g_0=1.19\times10^{20}$ $eV^{-1}cm^{-3}$ for $x_S=0.14$. The donor-bound exciton line is located at $\varepsilon\simeq4$ meV and has a half width $\Delta E=2$ meV in the Se-rich alloy. This leads to integrated values of localized state densities in this energy band of 1.9×10^{17} cm^{-3} for $x_S=0.36$ and 6.4×10^{15} cm^{-3} for $x_S=0.14$ which should be compared to a donor concentration around 10^{16} cm^{-3}. We conclude that in the first case, excitons are predominantly localized in potential fluctuations, while in the Se-rich sample, excitons are more probably bound to donor impurities. This result is obtained for $\varepsilon\sim4$ meV. For smaller ε energies in the Se-rich sample the intense line observed quite close to the free-exciton edge should be, in our opinion, attributed to excitons localized in a tail of short extension. Here the more probable type of localization is the third case of Sec. IV: localization of the exciton center of mass, because the condition (32) applies and $M\alpha_g^2>m_p^*\alpha_p^2$. At the luminescence peak ($\varepsilon\simeq0.5$ meV) (Ref. 7) the optimum well radius, given by (11a), is 218 Å, a value larger than the exciton Bohr radius, as it should be. Although excitons localized in such wide wells could be considered as quasifree, the localization is responsible for the high oscillator strength[19] which explains the high intensity of the luminescence line.

Similar considerations on excitons localized in short extension tails can be applied to $Zn_xCd_{1-x}S$ ($x\leq0.15$),[8] $Zn_xCd_{1-x}Se$ ($0<x<1$),[9] $Zn_xCd_{1-x}Te$ ($x\leq0.5$),[29] and perhaps also to the systems studied in Ref. 6.

VI. CONCLUSIONS

We have developed a simple model of the exciton density of states induced by composition fluctuations in semiconductor alloys. This model considers the different ways an exciton can be localized in potential wells—as a whole or through electron (hole) confinement—depending on the coefficients of variation of band edges with composition and on the effective-mass ratio. In this respect it is remarkable that a good modeling of the luminescence bands due to localized excitons is obtained in quite different alloys: $Zn_{0.97}Hg_{0.03}Te$ (electron localization), $CdS_{0.36}Se_{0.64}$ (hole localization), and $Cd_{0.92}Hg_{0.08}Te$ (exciton confinement). For the first time this type of fitting is quantitative in the sense that the predicted energy dependence of the density of states is quite well reproduced by the line-shape adjustment. The model could be refined by introducing the variation of the exciton binding energy with the potential well radius, which was neglected in this work. Some calculations have appeared for spherical wells of infinite depths[30] and for special quantum boxes.[31] They should be adapted to the present case. On the other hand, our formulation could now be used to study other exciton-related processes in alloys such as the dependence of luminescence upon excitation intensity, temperature and time.[32]

ACKNOWLEDGMENTS

One of us (D.O.) is grateful to the Algerian Ministry of Higher Education and Scientific Research [Ministère d'Enseignement et de la Recherche Scientifique (MERS)] for its financial support. We also thank R. Triboulet for providing us with the $Zn_{0.97}Hg_{0.03}Te$ sample.

[1]E. Cohen and M. D. Sturge, Phys. Rev. B **25**, 3828 (1982).
[2]S. Permogorov, A. Reznitsky, S. Verbin, G. O. Müller, P. Flögel, and M. Nikiforova, Phys. Status Solidi B **113**, 589 (1982).
[3]J. A. Kash, A. Ron, and E. Cohen, Phys. Rev. B **28**, 6147 (1983).
[4]S. Shevel, R. Fisher, E.O. Göbel, G. Noll, and P. Thomas, J. Lumin. **37**, 45 (1987).
[5]C. Gourdon and P. Lavallard, Phys. Status Solidi B **153**, 641 (1989).
[6]H. Mariette, Y. Marfaing, and J. Camassel, in *The Physics of Semiconductors*, edited by O. Engström (World Scientific, Singapore, 1987), p. 1405.
[7]C. Gourdon, P. Lavallard, S. Permogorov, and A. Reznitsky, J. Lumin. **39**, 269 (1988).
[8]L. G. Suslina, D. L. Fedorov, A. G. Areshkin, and V. G. Melekhin, Solid State Commun. **55**, 345 (1985).
[9]A. S. Nasibov, Y. V. Korostelin, P. V. Shapkin, L. G. Suslina, D. L. Fedorov, and L. S. Markov, Solid State Commun. **71**, 867 (1989).
[10]S. D. Baranovski and A. L. Efros, Fiz. Tekh. Poluprovodn. **2**, 2237 (1978) [Sov. Phys.—Semicond. **12**, 1328 (1978)].

[11]B. Halperin and M. Lax, Phys. Rev. **148**, 722 (1966).
[12]M. Oueslati, C. Benoit A La Guillaume, and M. Zouaghi, Phys. Rev. B **37**, 3037 (1988).
[13]I. M. Lifshitz, Adv. Phys. **13**, 483 (1964); Zh. Eksp. Teor. Fiz. **53**, 743 (1967) [Sov. Phys.—JETP **26**, 462 (1968)].
[14]J. Singh and K. K. Bajaj, Appl. Phys. Lett. **48**, 1077 (1986).
[15]Y. Merle D'Aubigné, Le Si Dang, A. Wasiela, N. Magnea, F. Dal'bo, and A. Million, J. Phys. (Paris) Colloq. **48**, C5-363 (1987).
[16]A. Messiah, *Mécanique Quantique* (Dunod, Paris, 1962), Vol. 1, p. 305.
[17]N. N. Ablyazov, A. G. Areshkin, V. G. Melekhin, L. G. Suslina, and D. L. Fedorov, Phys. Status Solidi B **135**, 217 (1986).
[18]A. Marbeuf, D. Ballutaud, R. Triboulet, H. Dexpert, P. Lagarde, and Y. Marfaing, J. Phys. Chem. Solids **50**, 975 (1989).
[19]E. I. Rashba and G. E. Gurgenishvili, Fiz. Tverd. Tela (Leningrad) **4**, 1029 (1962) [Sov. Phys.—Solid State **4**, 759 (1962)].
[20]A. Lusson, Ph.D. thesis, University of Paris VI, 1987.
[21]J. Camassel, J. P. Laurenti, A. Bouhemadou, R. Legros, A. Lusson, and B. Toulouse, Phys. Rev. B **38**, 3948 (1988).
[22]H. Mariette, R. Triboulet and Y. Marfaing, J. Cryst. Growth 86, 558 (1988).
[23]*Physics of II-VI and I-VII Compounds, Semimagnetic Semiconductors,* Subrol. b of *Semiconductors,* Vol. 17 of *Landolt-Börnstein, Functional Relationships in Science and Technology,* Group III, New Series, edited by K. H. Hellwege (Springer-Verlag, Berlin, 1982).
[24]T. M. Duc, C. Hsu, and J. P. Faurie, Phys. Rev. Lett. **58**, 1127 (1987).
[25]R. Legros and R. Triboulet, J. Cryst. Growth **72**, 264 (1985).
[26]W. A. Harrison, J. Vacuum Sci. Technol. **14**, 1016 (1977); R. K. Swank, Phys. Rev. **153**, 844 (1967).
[27]O. Goede, D. Henning, and L. John, Phys. Status Solidi B **96**, 671 (1979).
[28]A. Fried, A. Ron, and E. Cohen, Phys. Rev. B **39**, 5913 (1989).
[29]R. Legros, Y. Marfaing, and D. Ouadjaout (private communication).
[30]Y. Kayanuma, Phys. Rev. B **38**, 9797 (1988).
[31]G. W. Bryant, Phys. Rev. B **37**, 8763 (1988).
[32]M. Oueslati, C. Benoît á la Guillaume, and M. Zouaghi, J. Phys. Condens. Matter **1**, 7705 (1989).